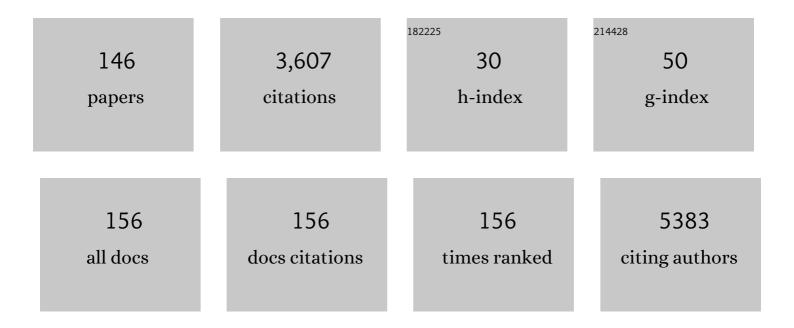
List of Publications by Year in descending order

Source: https://exaly.com/author-pdf/3271543/publications.pdf Version: 2024-02-01



WENRIN CHO

#	Article	IF	CITATIONS
1	Experimental Design for Time-Series RNA-Seq Analysis of Gene Expression and Alternative Splicing. Methods in Molecular Biology, 2022, 2398, 173-188.	0.4	2
2	Using a Simple Optical Management Layer to Solve the Contradiction between Efficiency and Transmittance for Semitransparent Organic Solar Cells. ACS Sustainable Chemistry and Engineering, 2022, 10, 2241-2247.	3.2	2
3	The value of genotype-specific reference for transcriptome analyses in barley. Life Science Alliance, 2022, 5, e202101255.	1.3	2
4	<scp>BaRTv2</scp> : a highly resolved barley reference transcriptome for accurate transcriptâ€specific <scp>RNA</scp> â€seq quantification. Plant Journal, 2022, 111, 1183-1202.	2.8	17
5	A high-resolution single-molecule sequencing-based Arabidopsis transcriptome using novel methods of Iso-seq analysis. Genome Biology, 2022, 23, .	3.8	35
6	Flexible Color Tunability and High Transmittance Semitransparent Organic Solar Cells. Solar Rrl, 2022, 6, .	3.1	9
7	3D RNA-seq: a powerful and flexible tool for rapid and accurate differential expression and alternative splicing analysis of RNA-seq data for biologists. RNA Biology, 2021, 18, 1574-1587.	1.5	58
8	Recent process of plasma effect in organic solar cells. Journal of Energy Chemistry, 2021, 52, 181-190.	7.1	6
9	Differential nucleosome occupancy modulates alternative splicing in <i>Arabidopsis thaliana</i> . New Phytologist, 2021, 229, 1937-1945.	3.5	19
10	Effective stability enhancement in ZnO-based perovskite solar cells by MACI modification. Journal of Materials Chemistry A, 2021, 9, 12161-12168.	5.2	26
11	Using 4â€Chlorobenzoic Acid Layer Toward Stable and Lowâ€Cost CsPbl 2 Br Perovskite Solar Cells. Solar Rrl, 2021, 5, 2100347.	3.1	4
12	Chromatin accessibility landscapes activated by cell-surface and intracellular immune receptors. Journal of Experimental Botany, 2021, 72, 7927-7941.	2.4	14
13	Strategies of modifying spiro-OMeTAD materials for perovskite solar cells: a review. Journal of Materials Chemistry A, 2021, 9, 4589-4625.	5.2	149
14	Cations Functionalized Carbon Nanoâ€Dots Enabling Interfacial Passivation and Crystallization Control for Inverted Perovskite Solar Cells. Solar Rrl, 2020, 4, 1900369.	3.1	16
15	Realizing efficiency improvement of polymer solar cells by using multi-functional cascade electron transport layers. Organic Electronics, 2020, 76, 105482.	1.4	5
16	Incorporating a Polar Molecule to Passivate Defects for Perovskite Solar Cells. Solar Rrl, 2020, 4, 1900489.	3.1	16
17	Performance improvement of planar perovskite solar cells with cobalt-doped interface layer. Applied Surface Science, 2020, 507, 145081.	3.1	22
18	Improving the performance of perovskite solar cells by surface passivation. Journal of Energy Chemistry, 2020, 46, 202-207.	7.1	31

#	Article	IF	CITATIONS
19	Recent Progress of Inverted Perovskite Solar Cells with a Modified PEDOT:PSS Hole Transport Layer. ACS Applied Materials & Interfaces, 2020, 12, 49297-49322.	4.0	88
20	Nonsense-Mediated RNA Decay Factor UPF1 Is Critical for Posttranscriptional and Translational Gene Regulation in Arabidopsis. Plant Cell, 2020, 32, 2725-2741.	3.1	42
21	Downy Mildew effector HaRxL21 interacts with the transcriptional repressor TOPLESS to promote pathogen susceptibility. PLoS Pathogens, 2020, 16, e1008835.	2.1	34
22	Efficiency enhancement in an inverted organic light-emitting device with a TiO ₂ electron injection layer through interfacial engineering. Journal of Materials Chemistry C, 2020, 8, 8206-8212.	2.7	5
23	Incorporating self-assembled silane-crosslinked carbon dots into perovskite solar cells to improve efficiency and stability. Journal of Materials Chemistry A, 2020, 8, 5629-5637.	5.2	23
24	The Effect of Drought on Transcriptome and Hormonal Profiles in Barley Genotypes With Contrasting Drought Tolerance. Frontiers in Plant Science, 2020, 11, 618491.	1.7	33
25	Alkali metal salts doped ZnO interfacial layers facilitate charge transport for organic solar cells. Organic Electronics, 2019, 74, 258-264.	1.4	11
26	Efficient perovskite solar cells enabled by ion-modulated grain boundary passivation with a fill factor exceeding 84%. Journal of Materials Chemistry A, 2019, 7, 22359-22365.	5.2	33
27	Alkali metal ions passivation to decrease interface defects of perovskite solar cells. Solar Energy, 2019, 193, 220-226.	2.9	8
28	Fullerene derivative layer induced phase separation and charge transport improvement for inverted polymer solar cells. Thin Solid Films, 2019, 690, 137559.	0.8	3
29	Highly efficient polymer solar cells based on low-temperature processed ZnO: application of a bifunctional Au@CNTs nanocomposite. Journal of Materials Chemistry C, 2019, 7, 2676-2685.	2.7	9
30	Colored semitransparent polymer solar cells with a power conversion efficiency of 9.36% achieved by controlling the optical Tamm state. Journal of Materials Chemistry A, 2019, 7, 4102-4109.	5.2	27
31	Using easily prepared carbon nanodots to improve hole transport capacity of perovskite solar cells. Materials Today Energy, 2019, 12, 161-167.	2.5	25
32	Surface Chlorination of ZnO for Perovskite Solar Cells with Enhanced Efficiency and Stability. Solar Rrl, 2019, 3, 1900154.	3.1	37
33	Using an easy interface passivation layer to improve performance of inverted polymer solar cells. Materials Letters, 2019, 250, 112-115.	1.3	1
34	Overcoming intrinsic defects of the hole transport layer with optimized carbon nanorods for perovskite solar cells. Nanoscale, 2019, 11, 8776-8784.	2.8	9
35	Facilitating electron extraction of inverted polymer solar cells by using organic/inorganic/organic composite buffer layer. Organic Electronics, 2019, 68, 187-192.	1.4	7
36	Cold-Dependent Expression and Alternative Splicing of Arabidopsis Long Non-coding RNAs. Frontiers in Plant Science, 2019, 10, 235.	1.7	70

#	Article	IF	CITATIONS
37	BaRTv1.0: an improved barley reference transcript dataset to determine accurate changes in the barley transcriptome using RNA-seq. BMC Genomics, 2019, 20, 968.	1.2	50
38	Developing 1D Sbâ€Embedded Carbon Nanorods to Improve Efficiency and Stability of Inverted Planar Perovskite Solar Cells. Small, 2019, 15, e1804692.	5.2	21
39	Facilitating electron collection of organic photovoltaics by passivating trap states and tailoring work function. Solar Energy, 2019, 181, 9-16.	2.9	6
40	High-Efficiency and High-Color-Rendering-Index Semitransparent Polymer Solar Cells Induced by Photonic Crystals and Surface Plasmon Resonance. ACS Applied Materials & Interfaces, 2018, 10, 6513-6520.	4.0	68
41	Simple Inverted Annealing Process to Improve Charge Transport Capability of Organic Photovoltaic Devices with Thick Active Layers. Journal of Physical Chemistry C, 2018, 122, 10706-10713.	1.5	4
42	How does temperature affect splicing events? Isoform switching of splicing factors regulates splicing of <i>LATE ELONGATED HYPOCOTYL</i> (<i>LHY</i>). Plant, Cell and Environment, 2018, 41, 1539-1550.	2.8	25
43	Boosting Electron Extraction in Polymer Solar Cells by Introducing a N-Type Organic Semiconductor Interface Layer. Journal of Physical Chemistry C, 2018, 122, 207-215.	1.5	8
44	A solution-processed binary cathode interfacial layer facilitates electron extraction for inverted polymer solar cells. Journal of Colloid and Interface Science, 2018, 514, 328-337.	5.0	6
45	Incorporating deep electron traps into perovskite devices: towards high efficiency solar cells and fast photodetectors. Journal of Materials Chemistry A, 2018, 6, 21039-21046.	5.2	8
46	Toward Efficient Carbon-Dots-Based Electron-Extraction Layer Through Surface Charge Engineering. ACS Applied Materials & Interfaces, 2018, 10, 40255-40264.	4.0	12
47	Using a facile processing method to facilitate charge extraction for polymer solar cells. Journal of Materials Chemistry C, 2018, 6, 11045-11051.	2.7	3
48	Rapid and Dynamic Alternative Splicing Impacts the Arabidopsis Cold Response Transcriptome. Plant Cell, 2018, 30, 1424-1444.	3.1	294
49	Employing Pentacene To Balance the Charge Transport in Inverted Organic Solar Cells. Journal of Physical Chemistry C, 2018, 122, 17110-17117.	1.5	6
50	Reducing charge recombination of polymer solar cells by introducing composite anode buffer layer. Solar Energy, 2018, 171, 8-15.	2.9	12
51	Efficient 4,4′,4″â€ŧris(3â€methylphenylphenylamino)triphenylamine (mâ€MTDATA) Hole Transport Layer in Perovskite Solar Cells Enabled by Using the Nonstoichiometric Precursors. Advanced Functional Materials, 2018, 28, 1803126.	7.8	29
52	Semi-transparent polymer solar cells with optical adjusting layers. Journal of Materials Chemistry C, 2018, 6, 9494-9500.	2.7	15
53	High-efficiency polymer solar cells with low temperature solution-processed SnO ₂ /PFN as a dual-function electron transporting layer. Journal of Materials Chemistry A, 2018, 6, 17401-17408.	5.2	33
54	Overcoming Defect-Induced Charge Recombination Loss in Organic Solar Cells by Förster Resonance Energy Transfer. ACS Sustainable Chemistry and Engineering, 2018, 6, 9699-9706.	3.2	6

#	Article	IF	CITATIONS
55	The role of polymer dots on efficiency enhancement of organic solar cells: Improving charge transport property. Optics Communications, 2017, 395, 127-132.	1.0	6
56	An easily prepared carbon quantum dots and employment for inverted organic photovoltaic devices. Chemical Engineering Journal, 2017, 315, 621-629.	6.6	33
57	Boosted Electron Transport and Enlarged Built-In Potential by Eliminating the Interface Barrier in Organic Solar Cells. ACS Applied Materials & Interfaces, 2017, 9, 8830-8837.	4.0	25
58	Improved Optical Field Distribution and Charge Extraction through an Interlayer of Carbon Nanospheres in Polymer Solar Cells. Chemistry of Materials, 2017, 29, 2961-2968.	3.2	8
59	A high quality Arabidopsis transcriptome for accurate transcript-level analysis of alternative splicing. Nucleic Acids Research, 2017, 45, 5061-5073.	6.5	262
60	Interface passivation and electron transport improvement of polymer solar cells through embedding a polyfluorene layer. Physical Chemistry Chemical Physics, 2017, 19, 15207-15214.	1.3	8
61	Decreased Charge Transport Barrier and Recombination of Organic Solar Cells by Constructing Interfacial Nanojunction with Annealing-Free ZnO and Al Layers. ACS Applied Materials & Interfaces, 2017, 9, 22068-22075.	4.0	28
62	Dual Roles of the Fullerene Interlayer on Light Harvesting and Electron Transfer for Highly Efficient Polymer Solar Cells. Journal of Physical Chemistry C, 2017, 121, 8722-8730.	1.5	4
63	An easily prepared Ag 8 GeS 6 nanocrystal and its role on the performance enhancement of polymer solar cells. Organic Electronics, 2017, 45, 247-255.	1.4	10
64	Annealing-Free ZnO:PEI Composite Cathode Interfacial Layer for Efficient Organic Solar Cells. ACS Photonics, 2017, 4, 2952-2958.	3.2	32
65	Barley SIX-ROWED SPIKE3 encodes a putative Jumonji C-type H3K9me2/me3 demethylase that represses lateral spikelet fertility. Nature Communications, 2017, 8, 936.	5.8	78
66	Orienting the Microstructure Evolution of Copper Phthalocyanine as an Anode Interlayer in Inverted Polymer Solar Cells for High Performance. ACS Applied Materials & Interfaces, 2017, 9, 32044-32053.	4.0	6
67	Enhanced Photovoltaic Performance of Tetrazine-Based Small Molecules with Conjugated Side Chains. ACS Sustainable Chemistry and Engineering, 2017, 5, 8684-8692.	3.2	10
68	Impedance investigation of the highly efficient polymer solar cells with composite CuBr ₂ /MoO ₃ hole transport layer. Physical Chemistry Chemical Physics, 2017, 19, 20839-20846.	1.3	25
69	TSIS: an R package to infer alternative splicing isoform switches for time-series data. Bioinformatics, 2017, 33, 3308-3310.	1.8	58
70	High sensitive and fast formaldehyde gas sensor based on Ag-doped LaFeO3 nanofibers. Journal of Alloys and Compounds, 2017, 695, 1122-1127.	2.8	102
71	High performance humidity sensor based on metal organic framework MIL-101(Cr) nanoparticles. Journal of Alloys and Compounds, 2017, 695, 520-525.	2.8	82
72	Improved performance of inverted polymer solar cells using Cd 2 SSe/ZnS quantum dots. Materials Letters, 2017, 188, 244-247.	1.3	1

#	Article	IF	CITATIONS
73	Improving the charge carrier transport of organic solar cells by incorporating a deep energy level molecule. Physical Chemistry Chemical Physics, 2017, 19, 245-250.	1.3	22
74	Magnetic coupling metasurface for achieving broad-band and broad-angular absorption in the MoS_2 monolayer. Optical Materials Express, 2017, 7, 100.	1.6	31
75	An organosilane self-assembled monolayer incorporated into polymer solar cells enabling interfacial coherence to improve charge transport. Physical Chemistry Chemical Physics, 2016, 18, 16005-16012.	1.3	5
76	Enhanced electron extraction capability of polymer solar cells via modifying the cathode buffer layer with inorganic quantum dots. Physical Chemistry Chemical Physics, 2016, 18, 11435-11442.	1.3	9
77	Small molecules based on tetrazine unit for efficient performance solution-processed organic solar cells. Solar Energy Materials and Solar Cells, 2016, 155, 30-37.	3.0	18
78	Versatile dual organic interface layer for performance enhancement of polymer solar cells. Journal of Power Sources, 2016, 333, 99-106.	4.0	17
79	Optimization of PDTS-DTffBT-Based Solar Cell Performance through Control of Polymer Molecular Weight. Journal of Physical Chemistry C, 2016, 120, 19513-19520.	1.5	8
80	Performance enhancement of organic photovoltaic devices enabled by Au nanoarrows inducing surface plasmonic resonance effect. Physical Chemistry Chemical Physics, 2016, 18, 24285-24289.	1.3	10
81	Employing inorganic/organic hybrid interface layer to improve electron transfer for inverted polymer solar cells. Electrochimica Acta, 2016, 210, 874-879.	2.6	4
82	Efficiency Improvement of Organic Solar Cells via Introducing Combined Anode Buffer Layer To Facilitate Hole Extraction. Journal of Physical Chemistry C, 2016, 120, 13954-13962.	1.5	16
83	Preparation and employment of carbon nanodots to improve electron extraction capacity of polyethylenimine interfacial layer for polymer solar cells. Organic Electronics, 2016, 33, 62-70.	1.4	13
84	Enhanced Electron Extraction Capability of Polymer Solar Cells via Employing Electrostatically Self-Assembled Molecule on Cathode Interfacial Layer. ACS Applied Materials & Interfaces, 2016, 8, 8224-8231.	4.0	29
85	Performance Improvement of Polymer Solar Cells by Surface-Energy-Induced Dual Plasmon Resonance. ACS Applied Materials & Interfaces, 2016, 8, 6183-6189.	4.0	46
86	Unique Gold Nanorods Embedded Active Layer Enabling Strong Plasmonic Effect To Improve the Performance of Polymer Photovoltaic Devices. Journal of Physical Chemistry C, 2016, 120, 6198-6205.	1.5	32
87	Employing Easily Prepared Carbon Nanoparticles To Improve Performance of Inverted Organic Solar Cells. ACS Sustainable Chemistry and Engineering, 2016, 4, 2359-2365.	3.2	16
88	Enhanced toluene sensing performance of gold-functionalized WO 3 ·H 2 O nanosheets. Sensors and Actuators B: Chemical, 2016, 223, 761-767.	4.0	58
89	At RTD – a comprehensive reference transcript dataset resource forÂaccurate quantification of transcriptâ€specific expression in Arabidopsis thaliana. New Phytologist, 2015, 208, 96-101.	3.5	50
90	Improved color rendering index of low band gap semi-transparent polymer solar cells using one-dimensional photonic crystals. RSC Advances, 2015, 5, 54638-54644.	1.7	14

#	Article	IF	CITATIONS
91	Improving the efficiency of inverted polymer solar cells by introducing inorganic dopants. Physical Chemistry Chemical Physics, 2015, 17, 7960-7965.	1.3	20
92	Improved Power Conversion Efficiency of Inverted Organic Solar Cells by Incorporating Au Nanorods into Active Layer. ACS Applied Materials & amp; Interfaces, 2015, 7, 15848-15854.	4.0	20
93	Efficiency Improvement of Inverted Organic Solar Cells via Introducing a Series of Polyfluorene Dots in Electron Transport Layer. Journal of Physical Chemistry C, 2015, 119, 16462-16467.	1.5	2
94	Highly Efficient Semitransparent Polymer Solar Cells with Color Rendering Index Approaching 100 Using One-Dimensional Photonic Crystal. ACS Applied Materials & Interfaces, 2015, 7, 9920-9928.	4.0	81
95	Unraveling the effect of polymer dots doping in inverted low bandgap organic solar cells. Physical Chemistry Chemical Physics, 2015, 17, 16086-16091.	1.3	6
96	The role of phosphor nanoparticles in high efficiency organic solar cells. Synthetic Metals, 2015, 204, 65-69.	2.1	9
97	Highly Efficient Low-Bandgap Polymer Solar Cells with Solution-Processed and Annealing-Free Phosphomolybdic Acid as Hole-Transport Layers. ACS Applied Materials & Interfaces, 2015, 7, 5367-5372.	4.0	52
98	Enhancing the light-harvesting and charge transport properties of polymer solar cells by embedding NaLuF ₄ :Yb,Tm nanorods. RSC Advances, 2015, 5, 32891-32896.	1.7	8
99	The Performance Enhancement of Polymer Solar Cells by Introducing Cadmium-Free Quantum Dots. Journal of Physical Chemistry C, 2015, 119, 26747-26752.	1.5	25
100	The operation mechanism of poly(9,9-dioctylfluorenyl-2,7-diyl) dots in high efficiency polymer solar cells. Applied Physics Letters, 2015, 106, .	1.5	4
101	Surface Plasmon Resonance Enhanced Polymer Solar Cells by Thermally Evaporating Au into Buffer Layer. ACS Applied Materials & Interfaces, 2015, 7, 18866-18871.	4.0	45
102	The Role of Fe ₃ O ₄ Nanocrystal Film in Bilayer-Heterojunction CuPc/C ₆₀ Solar Cells. Journal of Nanoscience and Nanotechnology, 2014, 14, 3623-3626.	0.9	0
103	The role of Au nanorods in highly efficient inverted low bandgap polymer solar cells. Applied Physics Letters, 2014, 105, 223305.	1.5	12
104	Preparation and Ethanol Sensing Properties of In ₂ O ₃ Nanotubes. Journal of Nanoscience and Nanotechnology, 2014, 14, 3653-3657.	0.9	5
105	Photovoltaic Properties of Zr _{<i></i>} Ti _{1–<i>x</i>} O _{2&l Solid Solution Nanowire Arrays. Journal of Nanoscience and Nanotechnology, 2014, 14, 3731-3734.}	:; /S.l dB>	; 2
106	Solar-Blind Photodetector Based on LaAlO ₃ with Low Dark Current. Journal of Nanoscience and Nanotechnology, 2014, 14, 3827-3830.	0.9	5
107	Improving charge transport property and energy transfer with carbon quantum dots in inverted polymer solar cells. Applied Physics Letters, 2014, 105, .	1.5	42
108	The action mechanism of TiO2:NaYF4:Yb3+,Tm3+ cathode buffer layer in highly efficient inverted organic solar cells. Applied Physics Letters, 2014, 105, 053301.	1.5	5

#	Article	IF	CITATIONS
109	Application of Solution-Processed V ₂ O ₅ in Inverted Polymer Solar Cells Based on Fluorine-Doped Tin Oxide Substrate. Journal of Nanoscience and Nanotechnology, 2014, 14, 4214-4217.	0.9	10
110	The role of NaYF4nanoparticles in inverted polymer solar cells. , 2014, , .		0
111	Light harvesting enhancement toward low IPCE region of semitransparent polymer solar cells via one-dimensional photonic crystal reflectors. Solar Energy Materials and Solar Cells, 2014, 127, 27-32.	3.0	24
112	Highly efficient and high transmittance semitransparent polymer solar cells with one-dimensional photonic crystals as distributed Bragg reflectors. Organic Electronics, 2014, 15, 470-477.	1.4	45
113	Efficiency enhancement of inverted organic solar cells by introducing PFDTBT quantum dots into PCDTBT:PC71BM active layer. Organic Electronics, 2014, 15, 2632-2638.	1.4	15
114	The light trapping enhancement of inverted polymer solar cells by introducing NaYF4 nanoparticles. Synthetic Metals, 2014, 195, 117-121.	2.1	7
115	Performance improvement of inverted polymer solar cells thermally evaporating CuI as an anode buffer layer. Synthetic Metals, 2014, 198, 1-5.	2.1	15
116	Efficiency enhancement of inverted polymer solar cells by doping NaYF4:Yb3+, Er3+ nanocomposites in PCDTBT:PCBM active layer. Solar Energy Materials and Solar Cells, 2014, 124, 126-132.	3.0	29
117	V-doped In2O3 nanofibers for H2S detection at low temperature. Ceramics International, 2014, 40, 6685-6689.	2.3	55
118	Highly efficient ITO-free polymer solar cells based on metal resonant microcavity using WO3/Au/WO3 as transparent electrodes. Organic Electronics, 2014, 15, 1545-1551.	1.4	23
119	The Short Circuit Current Improvement in P3HT:PCBM Based Polymer Solar Cell by Introducing PSBTBT as Additional Electron Donor. Journal of Nanoscience and Nanotechnology, 2014, 14, 3446-3449.	0.9	1
120	Characterization and Humidity Sensing Properties of the Sensor Based on Na ₂ Ti ₃ O ₇ Nanotubes. Journal of Nanoscience and Nanotechnology, 2014, 14, 4303-4307.	0.9	17
121	Simulation and Analysis of Terahertz Modulator Based a Gated Nanostructure. Journal of Nanoscience and Nanotechnology, 2014, 14, 3403-3406.	0.9	0
122	Role of solution-processed V2O5 in P3HT:PCBM based inverted polymer solar cells. Synthetic Metals, 2013, 170, 7-10.	2.1	10
123	The role of Ag nanoparticles in inverted polymer solar cells: Surface plasmon resonance and backscattering centers. Applied Physics Letters, 2013, 102, .	1.5	26
124	Sodium Titanate Nanorod Moisture Sensor and Its Sensing Mechanism. IEEE Electron Device Letters, 2013, 34, 1424-1426.	2.2	3
125	Analysis of plasma waves resonant detection for terahertz radiation in high mobility field effect transistor. Optik, 2013, 124, 6408-6410.	1.4	0
126	Performance improvement of inverted polymer solar cells by doping Au nanoparticles into TiO2 cathode buffer layer. Applied Physics Letters, 2013, 103, .	1.5	23

#	Article	IF	CITATIONS
127	Performance Improvement of Low-Band-Gap Polymer Solar Cells by Optical Microcavity Effect. IEEE Electron Device Letters, 2013, 34, 87-89.	2.2	8
128	Semitransparent polymer solar cells with one-dimensional (WO3/LiF)N photonic crystals. Applied Physics Letters, 2012, 101, .	1.5	37
129	Open-circuit voltage enhancement of inverted polymer bulk heterojunction solar cells by doping NaYF4 nanoparticles/PVP composites. Journal of Materials Chemistry, 2012, 22, 22382.	6.7	32
130	Semitransparent inverted polymer solar cells using MoO3/Ag/V2O5 as transparent anodes. Solar Energy Materials and Solar Cells, 2012, 97, 59-63.	3.0	40
131	The Study of Transmission Characteristics of a 17×17 All Fluorinated Polyimide Arrayed Waveguide Grating Multiplexer. , 2011, , .		1
132	Comparative study of field-effect mobility with different expressions in organic thin film transistors. Optik, 2009, 120, 668-672.	1.4	3
133	Water-soluble poly(3,4-ethylenedioxythiophene)/nano-crystalline TiO2 heterojunction solar cells. Microelectronics Journal, 2008, 39, 1683-1686.	1.1	2
134	Influence of TiO2 thin film morphology on the performance of polyaniline/TiO2 solar cells. , 2008, , .		0
135	Analysis and extraction of contact resistance in pentacene thin film transistors. , 2008, , .		0
136	Affect on the UV polymerization condition of polymer liquid crystal materials for variable optical attenuator. , 2008, , .		0
137	Performance improvement of TiO2â^•P3HT solar cells using CuPc as a sensitizer. Applied Physics Letters, 2008, 92, 073307.	1.5	67
138	p–n Heterojunction diodes made by assembly of ITO/nano-crystalline TiO2/polyaniline/ITO. Synthetic Metals, 2006, 156, 414-416.	2.1	26
139	Study of dynamic response on a MOEMS 2x2 optical switch. , 2005, 5625, 386.		0
140	Study on actuating voltage and switching time of a MOEMS optical switch. Optics and Laser Technology, 2005, 37, 601-607.	2.2	3
141	New method of optical variable attenuator with polymer-network liquid crystals. , 2004, , .		0
142	Transparent ITO electrode in the polymer network liquid crystal variable optical attenuator. , 2004, 5280, 397.		0
143	Optimization and fabrication of a polymeric-arrayed waveguide grating multiplexer. , 2002, , .		0

144 Optimization of polymer-arrayed waveguide grating multiplexer. , 2001, 4603, 278.

0

#	Article	IF	CITATIONS
145	Design and loss characteristics of an 8x8 polymer arrayed-waveguide grating multi/demultiplexer. , 2001, , .		Ο
146	High-temperature characteristics of 1.55-μm InGaAs/InGaAsP strain-compensated multiple-quantum-well lasers. , 2001, , .		1